

Development of optimal weight algorithm for efficient application of dual tree complex wavelet transform for resolution enhancement of satellite images

Akanksha Garg, Deepak Murugan and Dharmendra Singh*

Department of Electronics and Communication Engineering,
Indian Institute of Technology, Roorkee 247 667, India

Wavelets have been intensively studied for resolution enhancement of images since the last decade. Subbands of decomposed wavelet images are interpolated and combined using equal weights to form resolution-enhanced images. Using different weights for subbands may provide different information content in the output image. Hence, the weights need to be optimized. Therefore, here a technique is proposed to obtain optimal weight for subbands in dual tree complex wavelet transform for resolution enhancement of satellite images. The proposed approach effectively selects the optimal weights of individual subbands automatically according to the variances of each subband, and achieves better image quality. The technique is applicable on different satellite data, like MODIS and PALSAR.

Keywords: DT-CWT, optimal weights algorithm, resolution enhancement, satellite images, wavelets.

HIGH spatial resolution satellite images are needed for various applications like, urban vegetation cover analysis¹, riparian and forest ecosystem classification², seismic risk assessment³, crop classification, etc., but their acquisition is usually expensive. Therefore, it is a requisite to develop and use a reliable resolution enhancement technique in order to get cost-effective high-resolution data. There are substantial research efforts bestowed to resolution enhancement of images such as interpolation-based and wavelets-based⁴⁻⁶, which proved successful to a certain extent. Resolution enhancement of an image is still a challenging task since the traditional resolution enhancement methods are found to suffer from limitations like loss of edges (i.e. high-frequency components), presence of artefacts in an image, etc. Preserving the edges and reduction of artefacts is crucial for the improvement of quality of an image⁷. Broadly, resolution enhancement is carried out in two ways⁸ – learning-based and reconstruction-based. The disadvantage of the learning-based method is that it requires a learning dictionary for enhancement, whereas reconstruction-based algorithms are better since they do not use such a dictionary and

address aliasing artefacts also; but still it is difficult to get effective outcomes as they usually suffer from noises. It is a critical task to enhance the resolution optimally so that error/noise can be suppressed. For that purpose, optimal reconstruction of the enhanced image in the transformed domain (wavelet domain) using weighting factors might play a significant role; but it is a challenging research problem. Currently, few studies have been reported on weight distribution⁹⁻¹⁶, but still there is a need to focus on optimal reconstruction to achieve resolution-enhanced images.

Recently, with the introduction of dual tree complex wavelet transform (DT-CWT)^{7,17,18}, it is found to be the most efficient method for resolution enhancement of satellite images¹⁹. It is nearly shift-invariant and directionally selective, consequently reducing much artifacts in the image. Basically, these characteristics of DT-CWT indicate that the accurate measure of spectral energy is provided by the squared magnitude of a given complex wavelet coefficient at a specific position in scale, space and orientation. Therefore, DT-CWT is used to decompose an input image into different subbands; but researchers were giving equal weights to all of them. Every subband possesses different levels of information. So, if information of subbands could be optimized, then there is a possibility of getting better results. Hence, there is a strong need to critically analyse the subbands. Therefore, in this study, we endeavour to make the properties of DT-CWT much finer by analysing and optimizing some parameters for preferred resolution enhancement.

The study presents a novel resolution enhancement technique which is derived from optimal weighted DT-CWT. It automatically estimates the weighting factors of individual high-frequency (HF) subbands obtained after decomposition of an image using DT-CWT in real time. Optimal weights are calculated according to the variances of the respective subbands. This type of weighting method has been used for different sensors²⁰, but still very less work has been reported for the subbands. Variance-based method is a good technique as it will be data-independent. It infers that as image statistics (i.e. variance) changes with the image from different date/scene/sensor data, the variance will automatically compute the required weights without the requirement of any a priori parameter. Variance generally represents the mean square error which is further minimized in order to reduce overall error in the image. Hence the optimal weighting factors play an important role in enhancement by de-emphasizing the noise present in the subbands. Therefore, in the proposed technique, the effective reconstruction of the image is performed based on the optimal weighted HF subbands, so that a sharper enhanced image could be achieved.

The study and experiments for resolution enhancement techniques have been performed on four different datasets. These are HH polarized image of ALOS PALSAR

*For correspondence. (e-mail: dharmfec@gmail.com)

Table 1. Details of the datasets used

Dataset	Test image	Acquisition date	Resolution (m)	No. of pixels (dimensions of image)
I	HH Polarized PALSAR	12 April 2011	25	200 × 200
II	MODIS band 1	7–14 April 2011	500	200 × 200
III	MODIS band 2	7–14 April 2011	500	200 × 200
IV (for validation)	MODIS band 2	7–14 April 2011	250	200 × 200

(Advanced Land Observation Satellite Phased Array L-band Synthetic Aperture RADAR) and bands 1 and 2 of the freely available MODIS (Moderate Resolution Imaging Spectroradiometer) dataset respectively. Dataset IV, i.e. Band 2 of MODIS with spatial resolution of 250 m has been used for validation; Table 1 provides the details.

DT-CWT with weights has been applied, and then experiments for sensitivity analysis of weights on the image have been carried out.

When DT-CWT is applied on an image, it provides different low-frequency (LF) and HF subbands. Generally, researchers reconstruct the enhanced image by giving equal weights to all the subbands, but each of the subbands may possess different information. In the earlier study²¹, sensitivity analysis was carried out to check the weight response for each subband, which if varied showed a change in the overall accuracy. The overall accuracy is found to be sensitive with respect to weight factor provided for resolution enhancement of images. It appears to increase as the weight factor is changed from $[-0.5 \ 0.5]$ with the step size of 0.1, and then starts decreasing. Therefore, there is a need to analyse the changes more critically in the reconstructed image by assigning different weights to the subbands. Hence, there is some scope for enhancing the resolution of an image as discussed below.

In the proposed technique, DT-CWT is used to decompose a low-resolution image into different subband images. DT-CWT decomposes the signals into real and imaginary parts in the transformed (complex wavelet) domain in different directions utilizing the two trees of discrete wavelet transform (DWT)¹⁷. Two complex-valued LF subbands and six complex-valued HF subbands are produced by a one-level DT-CWT of an image. Many features such as shift invariance and directional selectivity are offered by DT-CWT, unlike others (e.g. DWT). Owing to the directional selectivity of DT-CWT resolution enhancement is achieved, since HF details are contributed by the HF subbands present in six diverse orientations ($+75^\circ$, $+45^\circ$, $+15^\circ$, -15° , -45° and -75°)¹⁷.

In this study, reconstruction of a resolution-enhanced image has been carried out by assigning optimal weights to the subbands. However, a problem exists in the subband weighting approach which is the estimation of weighting factors. Neural networks are utilized by many researchers for nonlinear estimation of weights, but

information of any subband has not been utilized for weighting directly^{22,23}. Hence, this study focuses on utilizing information of subbands of an image for computation of weighting factors. The weights have been assigned according to the level of information carried by them individually. Thus, it has become possible to make the subbands more directionally selective, so that we can more selectively discriminate features of various orientations and de-emphasize the unreliable frequency subbands. Such weighting approach has many paybacks, such as simple computation, unbiased estimation being data-independent, and no need of any a priori parameter.

It is supposed that each of the subbands has different variance and this variance has a special role in reconstruction of the image. On the other hand, weighting factors are found to be inversely proportional to the variance of each subband²⁰. Henceforth, the optimal weighting factors are determined based on the estimation of variance of each subband. Basically, variances of subbands are needed to be minimized for getting the optimized weights.

Fourier and wavelet transforms are frequency domain methods which allow us to separately process the different frequency components of the image. However, Fourier analysis has some limitations, like it does not provide solution in both time and frequency domains simultaneously, and might take more time to complete the task²⁴. Thus wavelet transform has been utilized in this study to process an image in frequency domain as it overcomes the limitations of Fourier transform along with the ability of separately processing the HF components of the image, which are the prime causes of its superior performance. Henceforth, weight factors could also be employed separately on each of the HF subbands (HSB_i) obtained by applying wavelet transform on the image. Therefore, an attempt has been made in this study to modify the HF subbands by including the weight factors as follows

$$HSB_{w_i} = w_i * HSB_i, \quad i = 1, 2, 3, \dots, \quad (1)$$

where w_i is the weighting factor for subband i , HSB_i the HF subband i obtained directly after decomposition of an image using DT-CWT, and HSB is the weighted HF subband i .

This occurs due to the fact that the interpolation of the isolated HF subband images will preserve more HF

Table 2. Optimal weighting factors for all the datasets used

Optimal weights	Dataset I(a*)	Dataset I(b*)	Dataset II(a*)	Dataset II(b*)	Dataset III(a*)	Dataset III(b*)	Dataset IV
w_1	0.0600	0.0639	0.0475	0.0468	0.0530	0.0476	0.0722
w_2	0.1099	0.1118	0.0781	0.0921	0.0917	0.1116	0.0993
w_3	0.0597	0.0635	0.0491	0.0463	0.0486	0.0471	0.0723
w_4	0.1139	0.1051	0.0893	0.0904	0.0907	0.0926	0.0990
w_5	0.0526	0.0549	0.0545	0.0619	0.0598	0.0561	0.0364
w_6	0.0890	0.1034	0.0879	0.1034	0.0918	0.1048	0.0634
w_7	0.0502	0.0548	0.0534	0.0611	0.0570	0.0592	0.0334
w_8	0.0991	0.1093	0.1023	0.1168	0.1048	0.1104	0.0594
w_9	0.0680	0.0614	0.0833	0.0690	0.0782	0.0776	0.0921
w_{10}	0.1350	0.1223	0.1494	0.1341	0.1466	0.1063	0.1553
w_{11}	0.0648	0.0576	0.0859	0.0678	0.0779	0.0748	0.0933
w_{12}	0.0979	0.0920	0.1194	0.1105	0.0999	0.1117	0.1238

Note: a*, Respective dataset is down-sampled by a factor of 2. b*, Respective dataset is down-sampled by a factor of 4.

components than interpolating the input image directly⁷. Thus this experimentation has been carried out to preserve HF components more optimally by interpolating weighted HF components.

The proposed algorithm is implemented on an image to be enhanced in the following stepwise procedure:

(1) Read the input image (i.e. low resolution (LR) image) of size $m \times n$ (e.g. images I, II, III in Table 1).

(2) Apply DT-CWT on the input image: Six complex HF subbands and two complex LF subbands are obtained.

(3) Computation of optimal weights: This is performed in the following steps for each of the HF subbands of the image: (a) Calculate variance for each of the 12 HF subbands, i.e. real and imaginary parts of the obtained six HF subbands. For each individual subband i variance α_i^2 ($i = 1, 2, 3, \dots, 12$) is computed utilizing the following equation

$$\alpha_i^2 = \frac{1}{11} \left[11 * \text{Cov}(\text{HSB}_i, \text{HSB}_i) - \sum_{j=1, j \neq i}^{12} \text{Cov}(\text{HSB}_i, \text{HSB}_j) \right], \tag{2}$$

where $\text{Cov}(\text{HSB}_i, \text{HSB}_i)$ and $\text{Cov}(\text{HSB}_i, \text{HSB}_j)$ represent self-covariance of HSB_i and cross-covariance of HSB_i w.r.t. HSB_j .

(b) Determine the minimum of the variances of all HF subbands²⁰, i.e. α_{\min}^2 using the following equation

$$\alpha_{\min}^2 = \frac{1}{\sum_{i=1}^{12} \frac{1}{\alpha_i^2}}. \tag{3}$$

(c) Optimal weighting factors, i.e. w_i for each of the HF subbands are acquired by employing the following equation

$$w_i = \frac{\alpha_{\min}^2}{\alpha_i^2}. \tag{4}$$

Table 2 gives the weights obtained ($w_1 - w_2$) for all the input images to be enhanced. The optimal weights have been estimated in such a way that the sum of all the weights is 1.

(4) Modify the coefficients of the HF subbands by applying obtained weights on the respective HF subbands using eq. (1). Then weighted HF subbands will be obtained.

(5) Interpolate the HF subbands obtained from step 4 using Lanczos interpolation by a factor of f , and input image by a factor of $f/2$, where f is the resolution enhancement factor of the input image.

(6) Reconstruct the resolution enhanced image by employing inverse DT-CWT on the images obtained from step 5 i.e. interpolated weighted HF subbands and interpolated input image in order to achieve an output of resolution enhanced image (i.e. high resolution (HR) image) of size $fm \times fn$.

(7) Calculate PSNR (peak signal-to-noise ratio), RMSE (root mean square error), and correlation coefficient for performance assessment²⁵.

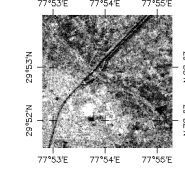
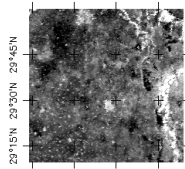
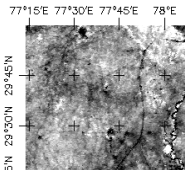
For example, let there be four subbands (LL, LH, HL and HH). Then the equations used to obtain optimal weights for all the four subbands will be as follows.

(1) Compute variance, i.e. $\alpha_1^2, \alpha_2^2, \alpha_3^2, \alpha_4^2$, for each of the subbands, LL, LH, HL and HH respectively (using eq. (2)) in the following manner

$$\alpha_1^2 = \frac{1}{3} [3 * \text{Cov}(\text{LL}, \text{LL}) - \text{Cov}(\text{LL}, \text{LH}) - \text{Cov}(\text{LL}, \text{HL}) - \text{Cov}(\text{LL}, \text{HH})],$$

$$\alpha_2^2 = \frac{1}{3} [3 * \text{Cov}(\text{LH}, \text{LH}) - \text{Cov}(\text{LH}, \text{LL}) - \text{Cov}(\text{LH}, \text{HL}) - \text{Cov}(\text{LH}, \text{HH})],$$

Table 3. Performance parameters for the data sets used

Dataset	Original image	Enhancement factor	Technique	PSNR (dB)	RMSE	Correlation coefficient
PALSAR (dataset I)		2x	Existing DT-CWT	27.0613	2.9766	0.73
			Proposed technique	28.8097	2.4339	0.80
		4x	Existing DT-CWT	25.1497	3.7094	0.58
			Proposed technique	26.4548	3.1919	0.65
MODIS band 1 (dataset II)		2x	Existing DT-CWT	45.7971	0.0083	0.84
			Proposed technique	48.0180	0.0064	0.90
		4x	Existing DT-CWT	43.3351	0.0110	0.72
			Proposed technique	44.8706	0.0092	0.79
MODIS band 2 (dataset III)		2x	Existing DT-CWT	45.3750	0.0087	0.81
			Proposed technique	47.3650	0.0069	0.87
		4x	Existing DT-CWT	42.9728	0.0114	0.66
			Proposed technique	44.4395	0.0097	0.73

$$\alpha_3^2 = \frac{1}{3} [3 * \text{Cov}(\text{HL}, \text{HL}) - \text{Cov}(\text{HL}, \text{LL}) - \text{Cov}(\text{HL}, \text{LH}) - \text{Cov}(\text{HL}, \text{HH})],$$

$$\alpha_4^2 = \frac{1}{3} [3 * \text{Cov}(\text{HH}, \text{HH}) - \text{Cov}(\text{HH}, \text{LL}) - \text{Cov}(\text{HH}, \text{LH}) - \text{Cov}(\text{HH}, \text{HL})].$$

(2) Compute minimum of the variances (using eq. (3))

$$\alpha_{\min}^2 = \frac{1}{\frac{1}{\alpha_1^2} + \frac{1}{\alpha_2^2} + \frac{1}{\alpha_3^2} + \frac{1}{\alpha_4^2}}.$$

(3) Calculation of weight factors (using eq. (4))

$$w_1 = \frac{\alpha_{\min}^2}{\alpha_1^2}, w_2 = \frac{\alpha_{\min}^2}{\alpha_2^2}, w_3 = \frac{\alpha_{\min}^2}{\alpha_3^2}, w_4 = \frac{\alpha_{\min}^2}{\alpha_4^2}.$$

(4) Obtain weighted subbands (using eq. (1))

$$\text{LL}_w = w_1 * \text{LL}, \text{LH}_w = w_2 * \text{LH},$$

$$\text{HL}_w = w_3 * \text{HL}, \text{HH}_w = w_4 * \text{HH}.$$

Experiments have been carried out on numerous satellite images: one high resolution satellite image, i.e. HH polarized PALSAR (dataset I), and two moderate resolution

satellite images, i.e. bands 1 and 2 of MODIS (dataset II and III). All the original images are displayed in Table 3, and Table 1 provides the details. To facilitate the efficacy of the proposed algorithm over the existing DT-CWT method, three images with different features are used for performance analysis. For comparing the results and computing the parameters, it is important that the output and reference image should be at the same scale. Consequently, original images are considered as reference images. Moreover, the input images, i.e. LR images (to be used as input for resolution enhancement) are obtained by down-sampling the original images by factors of 2 and 4, for further enhancement by the respective factors. Then the output enhanced (HR) image obtained will be of the same scale as the original image, which is the requisite for performance evaluation.

It was shown by Demiral and Anbarjafari⁷ that DT-CWT over-performs conventional interpolation and state-of-the-art methods. Moreover, Table 3 demonstrates the quantitative comparison of the proposed technique with enlargement factors of 2 and 4 on all the three images over the existing DT-CWT method in terms of PSNR, RMSE and correlation coefficient with reference to the original image²⁵. It is evident from Table 3 that the proposed technique presents better results in terms of the given performance parameters, indicating the quality of the enhanced image. First, good correlation is observed between the resolution-enhanced and original images (reference images), with an improvement of 6%–7% in correlation using the proposed technique compared to the

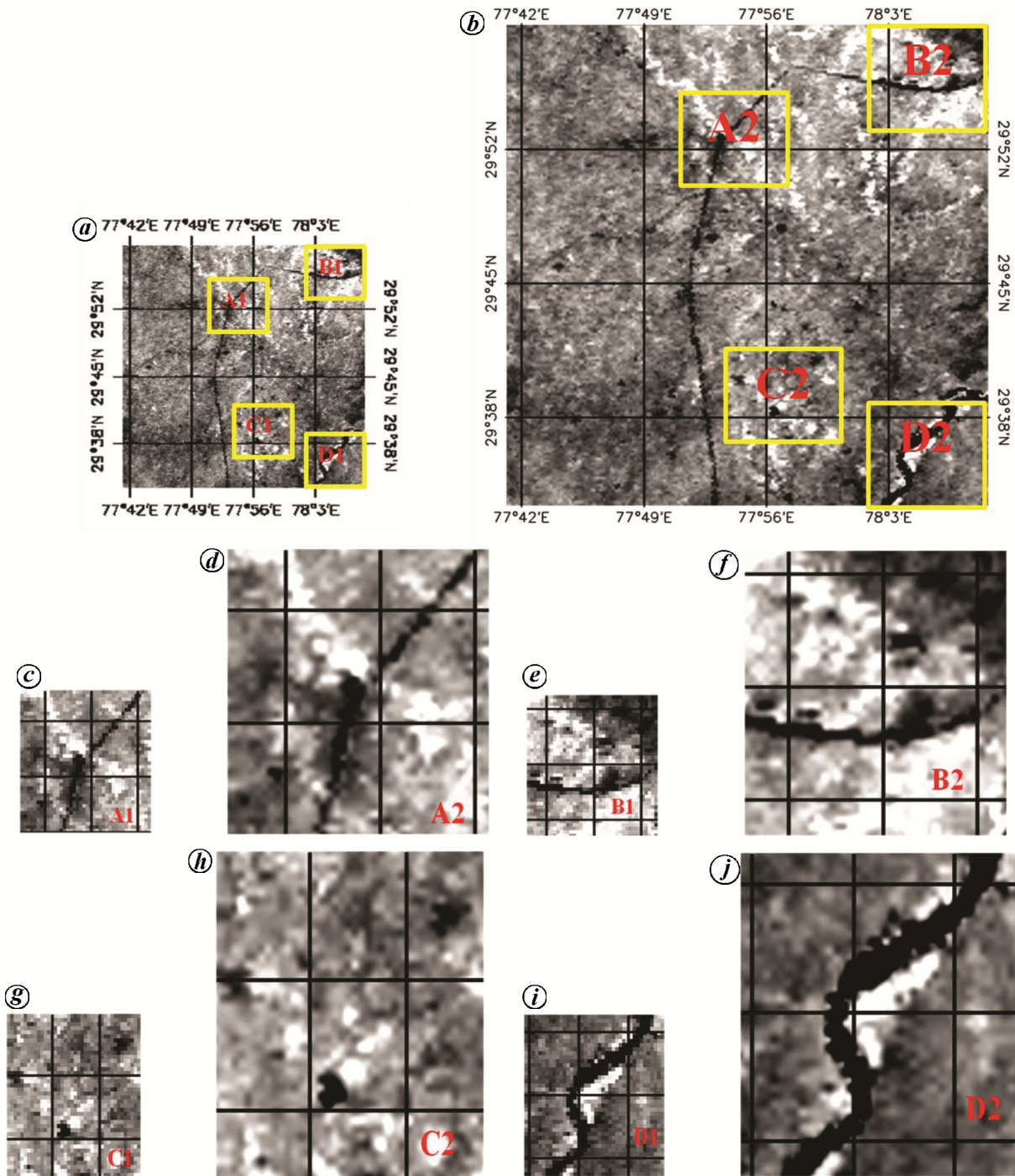


Figure 1. Dataset IV (MODIS band 2): *a*, original (LR) image; *b*, 10 times resolution enhanced (HR) image; *c*, zoomed-in image of highlighted area A1 of (*a*); *d*, Zoomed-in image of highlighted area A2 of (*b*); *e*, zoomed-in image of highlighted area B1 of (*a*); *f*, zoomed-in image of highlighted area B2 of (*b*); *g*, zoomed-in image of highlighted area C1 of (*a*); *h*, zoomed-in image of highlighted area C2 of (*b*); *i*, zoomed-in image of highlighted area D1 of (*a*); *j*, zoomed-in image of highlighted area D2 of (*b*). Note: A1, A2 represent the same area; B1, B2 represent the same area; C1, C2 represent the same area; D1, D2 represent the same area.

existing DT-CWT method. It simply infers that information content in the reconstructed image remains approximately the same as in the original image along with enhancement in the image quality. Using the proposed algorithm, PSNR also seems to be improved by 1.5–2.3 dB approximately, and RMSE is reduced for different

kinds of data compared to the other method. Higher PSNR and lower RMSE imply better image quality.

The proposed weighted DT-CWT-based resolution enhancement method suppresses more artifacts compared to the existing methods which can be clearly stated through the values of PSNR and other parameters given

in Table 3. The proposed technique is able to retain the desirable information because of exploitation of the properly weighted HF subbands. Hence, it is clear that the proposed weighted DT-CWT technique is superior to the existing DT-CWT method, because of the sensitivity of weights of HF subbands in enhancement, which in turn helps in significant improvement of the image quality.

For visual comparison, the original image of dataset IV, i.e. band 2 of MODIS with 250 m spatial resolution is used as input image (LR), and its resolution enhancement is carried out by a factor of 10 using the proposed algorithm. Figure 1 shows the original image (LR image), resolution enhanced (HR) image obtained, and zoomed-in images of their small highlighted areas. It is clear from the figure that the image obtained after enhancement is clear, of better quality, and connected visually than the corresponding original image. From the zoomed-in images displayed in Figure 1c–j, significant visual enhancement can be observed, and hence it validates the proposed technique successfully.

In this study, the role of optimal weights along with wavelet decomposition is proposed for the resolution enhancement of satellite images. Optimal weights are estimated using variance minimization approach. Effective reconstruction of the resolution enhanced image is carried out using the proposed optimal weighted DT-CWT technique. Better PSNR and correlation coefficient are achieved, and therefore, we get enhanced image quality. The technique is data-independent, since it is based on variance of subbands. The optimized transform is, consequently, a potentially valuable approach for resolution enhancement and the developed technique has the potential to be used for different kinds of data.

1. Chengqi, C., Bin, L. and Ting, M., The application of very high resolution satellite image in urban vegetation cover investigation: a case study of Xiamen City. *J. Geogr. Sci.*, 2003, **13**, 265–270.
2. Johansen, K., Coops, N. C., Gergel, S. E. and Stange, Y., Application of high spatial resolution satellite imagery for riparian and forest ecosystem classification. *Remote Sensing Environ.*, 2007, **110**, 29–44.
3. Yuan, Z. X. and Wang, L. M., Application of high-resolution satellite image for seismic risk assessment. In Proceedings of the 13th World Conference on Earthquake Engineering, Vancouver, BC, Canada, 1–6 August 2004, Paper No. 3454.
4. Temizel, A. and Vlachos, T., Wavelet domain image resolution enhancement using cycle-spinning. *Electron. Lett.*, 2005, **41**, 119–121.
5. Temizel, A., Image resolution enhancement using wavelet domain hidden Markov tree and coefficient sign estimation. In 2007 IEEE International Conference on Image Processing, San Antonio, TX, 2007, pp. V-381–V-384.
6. Garg, A., Naidu, S. V., Ahmed, T., Yahia, H. and Singh, D., Wavelet based resolution enhancement for low resolution satellite images. In 2014 9th International Conference on Industrial and Information Systems, 2014, pp. 1–5.
7. Demirel, H. and Anbarjafari, G., Satellite image resolution enhancement using complex wavelet transform. *IEEE Geosci. Remote Sensing Lett.*, 2010, **7**, 123–126.

8. Jebadurai, J. and Peter, J. D., SK-SVR: sigmoid kernel support vector regression based in-scale single image super-resolution. *Pattern Recognit. Lett.*, 2017, **94**, 144–153.
9. Bhat, S., Babu, R. D. R., Rangarajan, K. and K.a, R., An algorithm to estimate scale weights of complex wavelets for effective feature extraction in aerial images. *Def. Sci. J.*, 2014, **64**, 549–556.
10. Xu, L., Zhang, J. Q. and Yan, Y., A wavelet-based multisensor data fusion algorithm. *IEEE Trans. Instrum. Meas.*, 2004, **53**, 1539–1545.
11. Sun, T., Wu, F. and Gao, W., Accurately weighting subbands in temporal wavelet transform. In 2006 IEEE International Symposium on Circuits and Systems, Island of Kos, 2006, pp. 4, 3024.
12. Nasersharif, B. and Akbari, A., Application of wavelet transform and wavelet thresholding in robust sub-band speech recognition. In 12th European Signal Processing Conference, Vienna, 2004, pp. 345–348.
13. Wang, Y. and Ruan, Q., Dual-tree complex wavelet transform based local binary pattern weighted histogram method for palmprint recognition. *Comput. Inform.*, 2012, **28**, 299–318.
14. Ying, T., Debin, Z. and Baihuan, Z., Ear recognition based on weighted wavelet transform and DCT. In 26th Chinese Control and Decision Conference (2014 CCDC), 2014, pp. 4410–4414.
15. Hsu, W.-Y. and Sun, Y.-N., EEG-based motor imagery analysis using weighted wavelet transform features. *J. Neurosci. Methods*, 2009, **176**, 310–318.
16. Yoshida, H., Zhang, W., Cai, W., Doi, K., Nishikawa, R. M. and Giger, M. L., Optimizing wavelet transform based on supervised learning for detection of microcalcifications in digital mammograms. In Proceedings, International Conference on Image Processing, Washington, DC, USA, 1995, vol. 3, pp. 152–155.
17. Selesnick, I. W., Baraniuk, R. G. and Kingsbury, N. C., The dual-tree complex wavelet transform. *IEEE Signal Process. Mag.*, 2005, **22**, 123–151.
18. Celik, T. and Tjahjadi, T., Image resolution enhancement using dual-tree complex wavelet transform. *IEEE Geosci. Remote Sensing Lett.*, 2010, **7**, 554–557.
19. Narasimhan, K., Elamaran, V., Kumar, S., Sharma, K. and Abhishek, P. R., Comparison of satellite image enhancement techniques in wavelet domain. *Res. J. Appl. Sci. Eng. Technol.*, 2012, **4**, 5492–5496.
20. Gao, S., Zhong, Y. and Li, W., Random weighting method for multisensor data fusion. *IEEE Sensing J.*, 2011, **11**, 1955–1961.
21. Garg, A., Naidu, S. V., Gupta, S., Singh, D., Brodu, N. and Yahia, H., A novel approach for optimal weight factor of DT-CWT coefficients for land cover classification using MODIS data. In IEEE International Geoscience and Remote Sensing Symposium, Beijing, 2016, pp. 4528–4531.
22. Okawa, S., Bocchieri, E. and Potamianos, A., Multi-band speech recognition in noisy environments. In Proceedings of the IEEE International Conference on Acoustics, Speech and Signal Processing, 1998, vol. 2, pp. 641–644.
23. Cerisara, C. and Fohr, D., Multi-band automatic speech recognition. *Comput. Speech Lang.*, 2001, **15**, 151–174.
24. Dhakale, R. B., Jadhav, B. D. and Patil, P. M., Satellite image (multispectral) enhancement techniques in wavelet domain: an overview. *Int. J. Comput. Appl.*, 2015, **112**, 16–20.
25. Harish, K. and Singh, D., Quality assessment of fused image of MODIS and PALSAR. *Prog. Electromagn. Res. B*, 2010, **24**, 191–221.

ACKNOWLEDGEMENT. We thank the Indo-French Centre for Applied Mathematics for support.

Received 30 September 2017; revised accepted 8 August 2019

doi: 10.18520/cs/v117/i12/2034-2039